Noninvasive Monitoring of Target Gene Expression by Imaging Reporter Gene Expression in Living Animals Using Improved Bicistronic Vectors

Yanling Wang, PhD[1,2]; Meera Iyer, PhD[1,2]; Alexander J. Annala, PhD[3]; Steve Chappell, PhD[4]; Vincent Mauro, PhD[4]; and Sanjiv S. Gambhir, MD, PhD[1,2,5]

[1]The Crump Institute for Molecular Imaging, David Geffen School of Medicine at UCLA, Los Angeles, California; [2]Department of Molecular & Medical Pharmacology, David Geffen School of Medicine at UCLA, Los Angeles, California; [3]Cedars-Sinai Medical Center, Los Angeles, California; [4]Department of Neurobiology, Scripps Research Institute, Skaggs Institute for Chemical Biology, La Jolla, California; and [5]Department of Radiology, Bio-X Program, Stanford University School of Medicine, Stanford, California

Indirect, noninvasive imaging of therapeutic gene expression based on levels of reporter gene expression is a powerful tool to devise improved therapeutic strategies in cancer gene therapy. The use of bicistronic vectors carrying internal ribosome entry sites (IRESs) allows the coexpression of multiple gene products from the same promoter but leads to considerable attenuation of the downstream gene. In this study, we describe the use of 10 linked copies of the Gtx (homeodomain protein) IRES (abbreviated as SIRES) in place of the encephalomyocarditis (EMCV) IRES in mediating downstream reporter gene expression in cell culture and in vivo. **Methods:** We constructed several plasmid vectors carrying different upstream and downstream reporter genes (herpes simplex virus type I thymidine kinase [tk], firefly luciferase [fl], and *Renilla* luciferase [rl]) placed between EMCV IRES and SIRES segments. RL, FL, and TK enzyme activities in N2a, C6, and 293 cells transiently transfected with these vectors were found to be significantly higher for the SIRES vectors than for the EMCV IRES vectors. For in vivo experiments, 4 stably transfected N2a cell lines were implanted in nude mice. The mice were imaged for rl and fl gene expression using a charged-coupled device (CCD) camera. For bioluminescence and microPET imaging of downstream gene expression of fl and tk genes, respectively, mice carrying 4 stably transfected xenografts were imaged using the CCD camera and microPET. **Results:** In cell culture, using rl as the upstream gene, we demonstrate that the expression of the downstream tk gene is 12-fold greater using SIRES when compared with EMCV IRES. Furthermore, the expression of the 2 genes was highly correlated in N2a cells. In vivo bioluminescence imaging using 4 stably transfected N2a cell lines revealed increasing levels of rl and fl gene expression. Bioluminescence and microPET, respectively, of fl and tk reporter gene expression in nude mice bearing N2a tumor xenografts showed the gene expression mediated by SIRES to be 4- and 8-fold higher, respectively, than EMCV IRES. **Conclusion:** These findings support the use of SIRES bicistronic vectors for a better assessment of therapeutic gene expression based on reporter gene expression in living subjects.

Received Sep. 10, 2004; revision accepted Nov. 23, 2004.

For correspondence or reprints contact: Sanjiv S. Gambhir, MD, PhD, Stanford University School of Medicine, James H. Clark Center, 318 Campus Dr., 1E, Stanford, CA 94305-5427.

E-mail: sgambhir@stanford.edu

Key Words: bicistronic vectors; bioluminescence imaging; target gene expression

J Nucl Med 2005; 46:667–674

Successful delivery of therapeutic genes to the tissue of interest is a vital prerequisite in clinical gene therapy applications. One of the main limitations in cancer gene therapy protocols is efficient gene targeting to tumor cells. Knowledge of the location, magnitude, and persistence of gene expression will allow better optimization of gene therapy protocols. To accurately monitor the location, magnitude, and time variation of gene expression in living subjects, it is essential to develop tools for the in vivo evaluation of therapeutic gene delivery. In this context, the use of reporter gene imaging in vivo is rapidly emerging as a powerful tool to monitor gene expression. The use of imaging modalities such as PET and SPECT has played a vital role in evaluating gene expression in a noninvasive and repetitive manner (*1–3*). Other nonradionuclide methods such as bioluminescent imaging using optical reporter genes are also under active use for monitoring gene expression in vivo (*4,5*).

PET has unique advantages over other imaging modalities in that it offers increased sensitivity, high quantitative capability, and the ability to transition from animal models to human applications. For use with PET, reporter genes have been validated that can act in either of 2 ways: They encode proteins that metabolize positron-labeled substrates to products that get trapped in cells or bind a positron-labeled ligand to its receptor (*2,6*). The development of microPET technology has made it feasible to develop assays for imaging gene expression in small animal models (*7*). Strategies for imaging gene expression include direct and indirect approaches. Direct approaches involve imaging the transgene product directly either by binding of a radiolabeled ligand directly to the gene product or enzyme-specific trapping of a radiolabeled probe. We and others have dem-

onstrated using wild-type tk reporter gene that radiolabeled substrates can be selectively phosphorylated and trapped in tk-expressing cells (*2,8,9*). Improvements in the reporter gene–reporter probe system have led to the development of reporter genes with enhanced substrate affinity (mutant tk) and alternate substrates (*10,11*). Information about the exact location and magnitude of gene expression is highly useful in clinical trials for gene therapy. However, most therapeutic transgene products lack appropriate ligands that can be radiolabeled. It is also not feasible to synthesize and radiolabel a new probe for every new therapeutic gene being investigated. Therefore, indirect imaging assays using a reporter gene in combination with a therapeutic gene are used to predict the level of therapeutic gene expression based on the level of reporter gene expression, where the 2 genes are linked by one of several approaches. A summary of the different approaches is reviewed elsewhere (*12*).

The concept in the indirect imaging strategy is to demonstrate a constant and proportional relationship in the expression of the 2 transgenes over a wide range of expression levels. One of the approaches known as the bicistronic approach involves the insertion of an internal ribosomal entry site (IRES) between the 2 genes. This leads to transcription of the 2 genes into a single messenger RNA (mRNA) followed by translation into 2 different proteins. IRES sequences are generally found in the 5′ untranslated regions (UTRs) of cellular and viral mRNAs and facilitate cap-independent translation (*13,14*). This feature allows the coexpression of multiple genes from the same promoter making IRESs attractive for use in gene therapy vectors. Using this strategy, we have shown earlier that the expression of 2 cis-linked genes can be noninvasively imaged with microPET in living mice (*15*). We observed a very good correlation between the expression of the target gene rl or dopamine type 2 receptor (*D2R*) and a PET reporter gene (mutant tk). Tjuvajev et al. have described a similar approach to image the expression of tk and lacZ genes using radiolabeled 2′-fluoro-2′-deoxy-1-β-D-arabinofuranosyl-5-iodouracil (FIAU) and a γ-camera (*9*). One of the limitations in constructs using encephalomyocarditis (EMCV) IRES is that the expression of the downstream gene is often attenuated. In our earlier studies, we found that the activity of the tk gene (located downstream from the IRES) was lower than the activity driven by cytomegalovirus (CMV) promoter. The attenuation of the downstream gene places an increasing demand on sensitivity in the PET approach. Also, the use of EMCV IRES-containing bicistronic constructs necessitates placing the therapeutic gene upstream of the IRES sequence for robust expression.

Chappell et al. have demonstrated that the 196-nucleotide (nt) 5′ UTR of the Gtx homeodomain mRNA contains an IRES and that multiple nonoverlapping fragments of this 5′ UTR possess IRES activity (*16*). They identified a 9-nt segment in one of these fragments that functions independently as an IRES, and multiple copies of this segment lead to a synergistic increase in IRES activity. In continuation with our work using EMCV IRES-based bicistronic vectors, we have been exploring ways to increase the expression of the downstream cistron. In this context, we report the development of highly efficient coexpression vectors using multiple copies of the 9-nt Gtx IRES in place of EMCV IRES to augment the expression of the downstream gene and to enhance the sensitivity of the imaging assay. For the sake of convenience, the 9-nt segment IRES is termed super IRES and is abbreviated as SIRES. A schematic illustration of reporter gene imaging using SIRES-containing vectors is shown in Figure 1. For cell culture studies, the reporter genes placed upstream of SIRES were rl, fl, and D2R genes. The downstream gene was tk. For in vivo experiments, the upstream reporter gene was rl and the downstream genes were fl and tk. The expression of rl and fl genes was monitored using a cooled charge-coupled device (CCD) camera, and tk gene expression was imaged using microPET with 9-(4-^{18}F-fluoro-3-hydroxymethylbutyl)guanine (^{18}F-FHBG) as the reporter probe.

MATERIALS AND METHODS

Radiolabeled Compounds

8-^{3}H-Penciclovir (488.4 GBq/mmol [13.2 Ci/mmol]) was purchased from Moravek Biochemicals. ^{18}F-FHBG (specific activity, 185–370 GBq/mmol [5–10 Ci/μmol]) was synthesized by a modification of the procedure reported by Alauddin and Conti (*17*). Radiochemical purity, as determined by high-performance liquid chromatography (HPLC), was greater than 97%. ^{3}H-Spiperone (555 GBq/mmol [15 Ci/mmol]) was obtained from NEN.

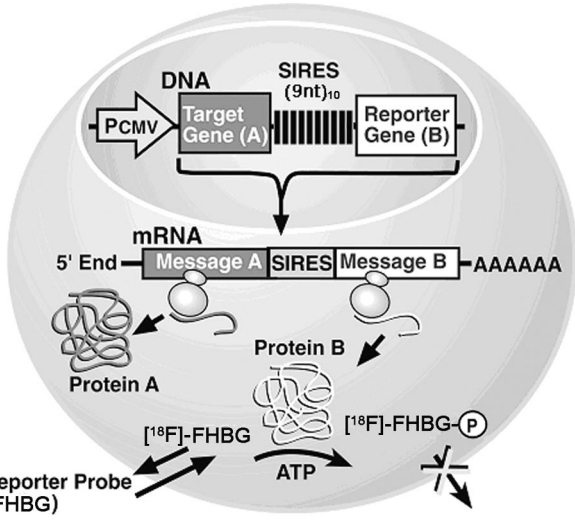

FIGURE 1. Schematic representation of imaging reporter gene expression using a SIRES-based bicistronic vector. Diagram illustrates how 2 proteins are expressed from the SIRES vector. Both gene A and gene B are coexpressed from the same vector and expression of gene B (a PET reporter) can be imaged quantitatively by trapping of a PET reporter probe (e.g., ^{18}F-FHBG), which will be an indirect measure of expression of gene A. PCMV = CMV promoter.

TABLE 1
IRES- and SIRES-Containing Plasmid Vectors Carrying Different Reporter Genes Used in This Study

Plasmid	pGL3 backbone
1	SV40-rl-IRES-tk (RIT)
2	SV40-rl-SIRES-tk (RST)
3	SV40-fl-IRES-tk (FIT)
4	SV40-fl-SIRES-tk (FST)
5	SV40-D2R-IRES-tk (DIT)
6	SV40-D2R-SIRES-tk (DST)
7	SV40-tk
8	SV40-fl (pGL3 control)
9	SV40-rl
10	SV40-D2R
11	CMV-D2R-IRES-tk (CDIT)
12	CMV-D2R-SIRES-tk (CDST)
13	CMV-D2R
14	CMV-tk
15	SV40-rl-IRES-fl (RIF)
16	SV40-rl-SIRES-fl (RSF)
	pcDNA3.1 backbone
17	CMV-D2R
18	CMV-tk
19	CMV-D2R-SIRES-tk

Construction of Plasmids

The list of plasmid vectors used in this study is shown in Table 1. Plasmids 1 and 2 were made by cloning in tk fragment, between *Nco* I and *Xba* I sites of plasmids 15 and 16 (*16*). The tk fragment was amplified from plasmid 18 (*15*) by polymerase chain reaction (PCR) (using primers 24 and 45). Plasmids 3 and 4 were made by cloning IRES-tk and SIRES-tk fragments between *Xba* I and *Bam*HI sites of pGL3 control vector (plasmid 8; Promega). For plasmids 5 and 6, the D2R fragment was cloned between *Nco* I and *Xba* I sites of plasmid 3 and 4. The D2R fragment was amplified from D2R/pCRII-TOPO by PCR primers 23 and 27 (*18*). Plasmids 7 and 10 were made by cloning PCR tk and D2R fragments into *Nco* I and *Xba* I sites of pGL3 control vector. Plasmid 9 was made by religating plasmid 15 after digestion with *Xba* I. Plasmid 17 was made by inserting the D2R fragment from D2R/pCRII-TOPO between the *Hin*dIII and *Xho* I sites of pcDNA3.1 vector. Plasmids 11 and 12 were made by cloning the pCMV-D2R fragment from plasmid 17 between *Bgl* II and *Xba* I sites of plasmids 3 and 4, respectively. Plasmids 13 and 14 were made by cloning the pCMV-D2R fragment from plasmid 17 and the pCMV-tk fragment from plasmid 18 (*15*) between *Xba* I and *Bgl* II sites of the pGL3 control vector. Plasmid 19 was made by cloning SIRES-tk fragment, which was amplified by PCR (primer YW3 and Yu 24) from plasmid 2, into *Not* I and *Xba* I sites of plasmid 17.

Cell Lines, Culture Conditions, and Transfection Procedures

N2a cells were a kind gift from Vincent Mauro's laboratory (Scripps Research Institute). N2a cells are murine neuroblastoma cells that were used in his laboratory to test the bicistronic vectors. They were grown in Dulbecco's modified Eagle medium (DMEM) medium (Invitrogen), supplemented with 10% fetal bovine serum (FBS), 0.2 mmol/L glutamine, 100 units/mL penicillin-G, and 100 mg/mL streptomycin. C6 is a rat glioma cell line that has been used in the Gambhir laboratory for several years. These cells were used as control cells to measure reporter gene uptake in C6 cells carrying the HSV1-sr39tk gene. C6 cells were grown in deficient DMEM (Irvine Scientific) supplemented with 5% FBS, 0.2 mmol/L glutamine, 100 units/mL penicillin-G, and 100 mg/mL streptomycin. 293 cells are human embryonic kidney cancer cells that are frequently used in transient transfection studies due to their high rate of transfection efficiency. 293 cells were obtained from the American Type Culture Collection and grown in MEM (Invitrogen), supplemented with 10% FBS, 100 units/mL penicillin-G, and 100 mg/mL streptomycin. The transfections were performed using Superfect transfection reagent (Qiagen). Transfection efficiencies were normalized by cotransfection with pCMV-β-gal plasmid (Clontech). The cells were harvested 48 h after transfection and assayed for the appropriate reporter enzyme activities. The vector used for stable transfection carried an antibiotic resistance gene (neomycin) that conferred resistance to geniticin (G418, a neomycin analog). The transformed cells carrying the plasmid vector were grown on plates containing G418 and only those cells that expressed the neomycin gene survived, thereby facilitating the selection of stable clones. Stable clones were selected with 500 μg/mL G418 and thereafter maintained at a concentration of 300 μg/mL.

Enzyme Assays

Renilla luciferase (RL) and firefly luciferase (FL) enzyme activities were measured using the Dual-Luciferase Reporter Assay System (Promega). Thymidine kinase (TK) enzyme activity was measured as described previously (*2*). D2R activity was determined using a modified version of the previously reported method (*6*). Cell culture homogenates were diluted to 200 μg/mL in assay solution. Samples were incubated with 2 nmol/L ^{3}H-spiperone in the absence and presence of 12.5 mmol/L (+)-butaclamol (ICN Biomedicals Inc.). The enzyme activities were normalized to the β-gal activities in the samples.

Bioluminescence Imaging of rl and fl Reporter Gene Expression In Vivo

Animal care and euthanasia were performed with the approval of the University of California Animal Research Committee. Six-week-old nude mice were anesthetized with ketamine/xylazine (4:1). The mice were implanted with 5×10^6 cells from 4 different stable clones (RSF). The 4 clones were selected from a group of 7 clones based on increasing levels of RL and FL enzyme activities from cell culture studies. Immediately after cell implantation, the mouse was injected with 100 μL of 0.2 μg/mL coelenterazine solution via tail vein and imaged immediately thereafter using the cooled CCD camera with an acquisition time of 1 min (*19*). Thirty minutes after imaging, the mouse was imaged again using D-luciferin (3 mg/mouse). Images were obtained using Living Image software (Xenogen) and Igor Image Analysis Software (Wavemetrics). For quantitation of transmitted light, regions of interest (ROIs) were drawn around the injection area and maximum relative light units were obtained. The bioluminescence signal is represented as photons/s/cm^2/steradian (sr).

microPET Imaging of Downstream tk Reporter Gene Expression In Vivo

Six-week-old nude mice were implanted with 2 N2a cell lines stably transfected with RIT and RST. When the tumors reached a size of 6 mm in diameter, the mice were injected with ^{18}F-FHBG (74 kBq/mouse [200 μCi/mouse]) and imaged using the micro-

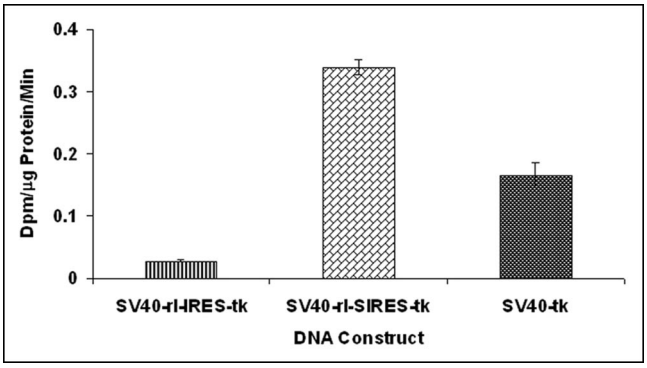

FIGURE 2. Plot of TK activity in N2a cells after transient transfection using 3 different plasmids (RIT, RST, and SV40-tk). For transfection experiments, 1.8 μg of each plasmid were cotransfected with 0.2 μg of pCMV-βgal into N2a cells in 6-well plates. Forty-eight hours later, cells were harvested and assayed for TK activity. Enzyme activities were normalized to β-gal activities. Error bars represent SE between triplicate samples.

PET. The mice were scanned in the prone position with the long axis of the mouse parallel to the long axis of the scanner. Scanning conditions were identical to those described earlier (*11*). After injection of the radiotracer, 60–90 min elapsed before starting image acquisition to allow for clearance of background activity. All images were reconstructed using an iterative reconstruction technique (*20*) and the ROIs were quantified as described earlier (*2*).

RESULTS

SIRES-Mediated Expression of Downstream tk Gene Is Significantly Greater than That of EMCV IRES

Table 1 lists the vectors used in the study. To determine if the expression of the downstream cistron is more robust in SIRES-containing vectors compared with EMCV IRES-containing vectors, N2a cells were transiently transfected with RIT and RST vectors. Analysis of TK enzyme activity 48 h after transfection shows SIRES-mediated activity of the downstream tk gene is 12-fold greater than that mediated by EMCV IRES (Fig. 2). Furthermore, the TK activity is observed to be significantly greater than that driven directly by the constitutive simian virus 40 (SV40) promoter ($P < 0.05$). We next evaluated TK enzyme activities in constructs in which the rl gene was replaced by fl and D2R genes both in EMCV IRES- and SIRES-containing vectors. The values for TK, D2R, RL, and FL activities are listed in Table 2. The results indicate that the downstream TK activities remain high irrespective of the nature of the upstream gene and are about 11-fold higher than the corresponding EMCV IRES vectors. These results clearly illustrate that the use of SIRES-containing bicistronic vectors leads to a significant enhancement in the expression of the gene placed downstream to SIRES (12-fold in RST, 16-fold in FST, and 11-fold in DST). The SIRES-driven expression of the downstream gene is robust and appears to be independent of the nature of the upstream gene. The RL and FL activities in these constructs also increased 7- and 2-fold, respectively, when compared with the EMCV IRES constructs. In constructs carrying the D2R gene, the D2R activity in both the SIRES- and IRES-containing vectors is observed to be low. However, when the SV40 promoter is replaced by a CMV promoter, we observe an increase in absolute D2R activities in both EMCV IRES- and SIRES-containing vectors, but the D2R activity in the SIRES construct is not significantly greater than that in the EMCV IRES construct (Table 3).

SIRES-Mediated Enhanced Expression of Downstream Cistron Is Preserved in Different Cell Lines

To evaluate whether SIRES exerts a similar effect on the activity of the downstream tk gene in different cell types, C6, N2a, and 293 cells were transiently transfected with different plasmids (RIT, RST, FIT, FST, DIT, DST, SV40-tk (Table 1). The presence of the SIRES sequence

TABLE 2
FL, RL, D2R, and TK Enzyme Activities in N2a Cells Transiently Transfected with Different Bicistronic Constructs Carrying EMCV IRES and SIRES Modules

Plasmid	pGL3 backbone	TK	D2R	RL	FL
1	SV40-rl-IRES-tk (RIT)	0.028		8.8	
2	SV40-rl-SIRES-tk (RST)	0.339		58.7	
3	SV40-fl-IRES-tk (FIT)	0.015			50.3
4	SV40-fl-SIRES-tk (FST)	0.234			96.9
5	SV40-D2R-IRES-tk (DIT)	0.03	0.3		
6	SV40-D2R-SIRES-tk (DST)	0.343	0.5		
7	SV40-tk	0.165			
8	SV40-fl				62.4
9	SV40-rl			21.3	
10	SV40-D2R		0.2		

Plasmids SV40-tk, SV40-D2R, SV40-rl, and SV40-fl were used as control vectors in transfections. FL and RL activities are expressed as RLU/μg protein. Units of D2R activity are pmol ^{3}H-spiperone bound/μg protein. TK activity is in units of dpm/mg protein/min. All enzyme activities were normalized to β-gal activity in each sample.

TABLE 3
D2R and TK Activities in N2a Cells Transfected with Constructs Carrying CMV and SV40 Promoters

Plasmid	pGL3 backbone	TK	D2R
5	SV40-D2R-IRES-tk (DIT)	0.03	0.3
6	SV40-D2R-SIRES-tk (DST)	0.343	0.5
11	CMV-D2R-IRES-tk (CDIT)	0.029	50.5
12	CMV-D2R-SIRES-tk (CDST)	0.29	73.7
13	CMV-D2R		58.1
14	CMV-tk	2.535	

between the 2 genes significantly enhanced the expression of the downstream cistron (tk) over that of IRES in all 3 cell lines (Fig. 3). Note that the TK activities are plotted on a logarithmic scale. These results are consistent with those reported by Chappell et al. (*16*) using a bicistronic construct with rl and fl as the 2 genes separated by a SIRES sequence. Since the fold increase using SIRES vectors was greatest in N2a cells, these cells were further used for transfection and isolation of stable clones carrying the bicistronic construct.

Expression of rl and tk Reporter Genes Is Highly Correlated in N2a Cells

In order for a bicistronic vector to be used for monitoring the expression of a therapeutic gene, it is essential to demonstrate a correlation between the expression of the reporter gene and the therapeutic gene. The present study entails the use of a second reporter gene in place of the therapeutic gene. N2a cells were transiently transfected with different concentrations of the RST plasmid. Analysis of RL and TK enzyme activities 48 h after transfection reveals significantly high levels of expression of the 2 genes. Furthermore, the rl and tk gene expression displays a high degree of correlation at all concentrations of DNA ($r^2 = 0.99$; Fig. 4A). The correlation was also maintained with the CDST plasmid, as illustrated by the D2R and TK activities in N2a cells ($r^2 = 0.92$; Fig. 4B). These 2 datasets demonstrate the

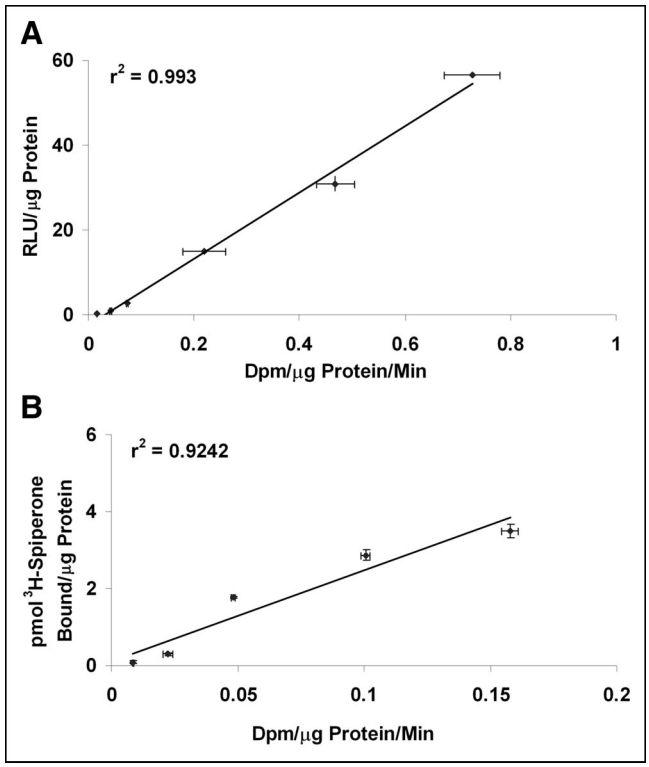

FIGURE 4. (A) Correlation of RL and TK activities from transient transfection assays in N2a cells. Cells were transfected with different concentrations of RST plasmid (2, 4, 5, 6, 8, and 10 μg). Forty-eight hours later, cells were harvested and assayed for RL and TK activities. RL and TK activities are represented as relative light units (RLU) per μg protein and dpm per μg protein per minute respectively. Error bars represent SE between triplicate observations. (B) Correlation of D2R and TK activities in transient transfection assays. Various amounts (2, 4, 5, 6, 8, and 10 μg) of CDST plasmid were transfected into N2a cells in 10-cm² dishes. Forty-eight hours later, cells were harvested and assayed for D2R and TK activities. D2R and TK activities are represented as picomoles of ³H-spiperone bound per μg of protein and dpm per μg protein per minute, respectively.

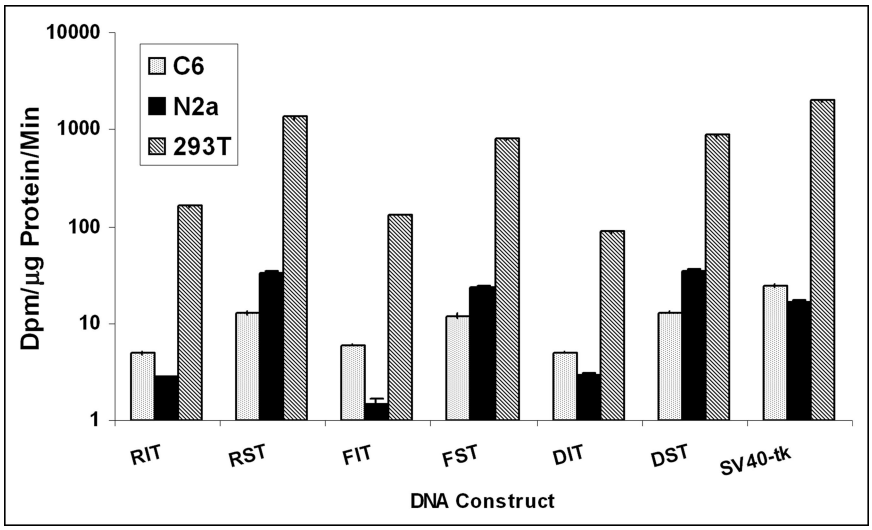

FIGURE 3. Plot of TK activity in different cell lines. N2a, C6, and 293T cells were transiently transfected with plasmids RIT, RST, FIT, FST, DIT, and DST. Plasmid SV40-tk was used as a positive control. Note that TK activities are represented on a logarithmic scale (based on 100-fold of dpm/μg protein/min). Error bars represent SE between triplicate samples.

ability to use the expression of the reporter gene as a measure of expression of the second transgene, which can be a therapeutic gene.

Optical Imaging of SIRES-Mediated rl and fl Reporter Gene Expression Demonstrates Good Correlation In Vivo

In transient transfections with N2a cells, we have demonstrated the significant enhancement in the expression of the gene positioned downstream of SIRES. To confirm that similar high levels of expression are maintained in N2a cells stably expressing the bicistronic construct, we generated 7 stable clones from N2a cells after transfection with RSF plasmid. The 7 cell lines were assayed for their RL and FL enzyme activities. They displayed varying levels of RL and FL activities, indicating moderate-to-high levels of expression. The differences in expression levels can be attributed to the number of copies of the gene that get stably inserted into the genome. The correlation between rl and fl gene expression was excellent ($r^2 = 0.96$; data not shown). Four different cell lines were selected, based on increasing levels of gene expression, and implanted subcutaneously in 4 different positions in a nude mouse. The mouse was imaged in the CCD camera immediately after cell implantation using coelenterazine and 30 min later using D-luciferin as substrates for rl and fl genes, respectively. Color images of visible light are superimposed on photographic images of mice with a scale in photons per second per square centimeter per steradian (sr). The 4 cell lines displayed increasing levels of bioluminescence signal (1–4; Fig. 5A) for rl and fl similar to that observed in cell culture. The bioluminescence signals (photons/s/cm^2/sr) for rl and fl were highly correlated ($r^2 = 0.98$; Fig. 5B).

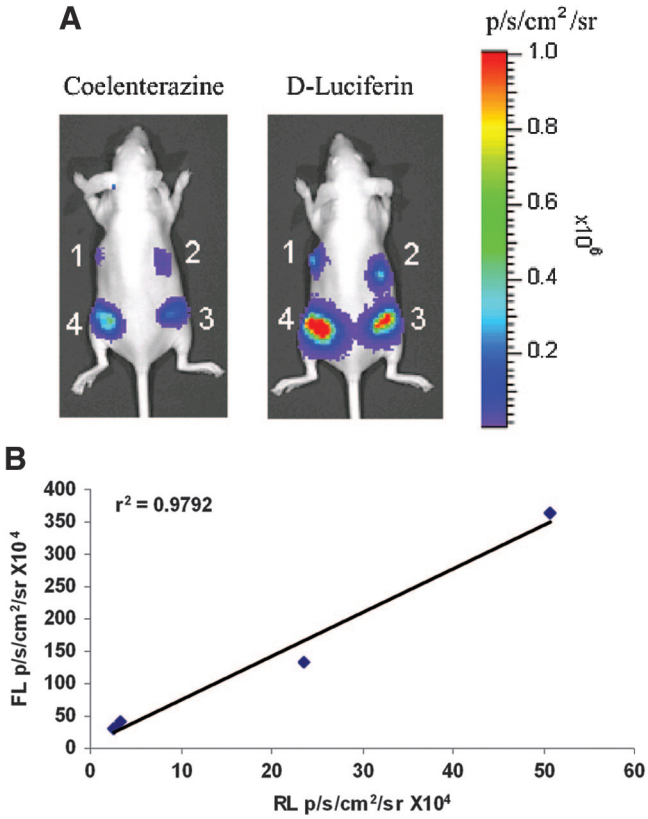

FIGURE 5. (A) Optical imaging of rl and fl reporter gene expression in vivo. Six-week old nude mice were implanted with 4 stably transfected N2a cell lines carrying RSF vector (with different levels of gene expression). Mice were imaged in CCD camera for rl expression immediately after cell implantation using coelenterazine (2 μg). Subsequent imaging was performed for fl expression using D-luciferin injected intraperitoneally (150 mg/kg). Signal intensity is represented as photons/s/cm^2/sr. (B) Correlation of RL and FL activities in stably transfected N2a cells. RLU for rl are plotted against corresponding light units for fl in the 4 N2a cell lines. Expression of the 2 reporter genes shows excellent correlation ($r^2 = 0.98$).

microPET Imaging of SIRES-Mediated Downstream tk Reporter Gene Expression Is Significantly Greater than That of EMCV IRES

In our earlier work with bicistronic vectors containing EMCV IRES, we observed strong attenuation of the downstream cistron (*15*). The SIRES-based bicistronic vectors evaluated in this study offer a convenient means to overcome this problem. To compare the levels of expression of the downstream gene using EMCV IRES and SIRES vectors, we imaged 2 nude mice, each carrying 4 N2a cell lines expressing varying levels of the transcript. The expression of fl gene is shown in Figure 6, left panel (EMCV IRES [RIF]), and Figure 6, middle panel (SIRES [RSF]). We found the bioluminescence signal in the SIRES-based vector to be significantly greater than the signal from the EMCV IRES mouse (signal intensities in xenografts 1–4 are 3.19×10^5, 4.01×10^5, 1.33×10^6, and 3.64×10^6 photons/s/cm^2/sr, respectively, for SIRES and 1.46×10^4, 1.76×10^4, 3.1×10^4, and 4.5×10^4 photons/s/cm^2/sr, respectively, for EMCV IRES). These results clearly illustrate the superiority of SIRES over EMCV IRES to augment the expression of the downstream gene. Similar high levels of expression were found when tk was used as the downstream gene in a bicistronic vector (Fig. 6, right panel). A nude mouse carrying N2a xenografts, RIT and RST on the left and right shoulders, respectively, was imaged using microPET with ^{18}F-FHBG reporter probe. The color scale (%ID/g) indicates the percentage injected dose that accumulates per gram of tumor. The SIRES xenograft shows a considerably high retention of the radiolabeled tracer compared with the xenograft carrying EMCV IRES (0.88 vs. 0.13 %ID/g tumor, respectively).

DISCUSSION

The goal in gene therapy imaging is to repetitively monitor the expression of the therapeutic gene(s) in living subjects. In this context, the use of vectors carrying multiple genes has particular importance. There are several approaches to link a reporter gene to a therapeutic gene and these are described in an earlier review (*12*). The use of an EMCV IRES allows for effective expression of 2 genes

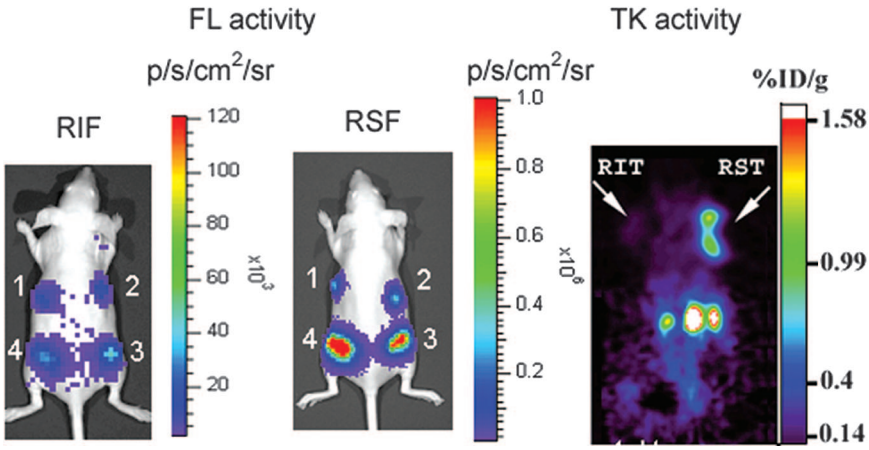

FIGURE 6. Optical and microPET imaging of fl and tk gene expression in vivo. For optical imaging of fl reporter gene expression, nude mice implanted with 4 different N2a cell lines (RIF, left panel; RSF, middle panel) were imaged in CCD camera immediately after cell implantation using D-luciferin (150 mg/kg). For tk gene imaging, nude mice carrying N2a tumor xenografts (RIT and RST on left and right shoulders, respectively; right panel) were imaged by microPET using ^{18}F-FHBG (74 kBq [200 μCi]). SIRES xenograft shows significantly higher retention of reporter when compared with EMCV IRES xenograft (0.88 vs. 0.13 %ID/g tumor, respectively).

from the same vector. We have reported earlier that 2 reporter genes can be linked using EMCV IRES and their expression can be noninvasively monitored using PET (*15*). However, we found that the expression of the gene placed downstream to EMCV IRES was considerably attenuated. This places substantial emphasis on the positioning of the target gene in the vector. For optimal expression, the target gene must be located upstream of EMCV IRES. However, this would compromise expression of the imaging reporter gene placed in the second cistron.

Chappell et al. have reported that a 9-nt fragment in the 5′ UTR of the Gtx homeodomain mRNA can function independently as an IRES sequence, leading to increased activities of the gene placed downstream of the 9-nt sequence (*16*). To address the issue of attenuation using EMCV IRES, we built a series of bicistronic vectors carrying 10 linked copies of the 9-nt segment (termed SIRES). We first compared the levels of reporter gene expression between EMCV IRES and SIRES in cell culture. Using an SV40 promoter, we demonstrated that the TK activity (downstream cistron) using the SIRES construct was significantly greater than that of the EMCV IRES. The SIRES activity was found to be independent of the nature of the cell type studied. Furthermore, the activity was 2-fold greater than that driven by SV40 promoter alone. In all of the vectors studied, SIRES-mediated TK activity was greater than that driven by the SV40 promoter. A comparison of expression levels between the imaging and target genes using different SIRES vectors showed excellent correlation, indicating simultaneous coexpression of the 2 genes.

The efficacy of SIRES-mediated gene expression in vivo was first demonstrated with fl reporter gene using N2a cells stably expressing RIF and RSF. In vivo bioluminescence imaging offers a powerful tool for the quantitative, real-time analysis of gene expression (*21,22*). It provides a low-cost, convenient, and sensitive alternative to PET for some applications. Bioluminescence imaging of fl gene expression immediately after cell implantation revealed a highly localized signal originating from the site of the cells. The level of fl reporter gene expression in SIRES cells was significantly greater than the corresponding signal from the EMCV IRES cells. The gene expression showed persistence with time up to 6 d. To determine whether the strong expression of the downstream gene was maintained using a different reporter gene, we used microPET to monitor the expression of the tk reporter gene in nude mice carrying N2a tumor xenografts (RIT and RST). SIRES-mediated tk gene expression was found to be 8-fold greater than that of EMCV IRES. These results support the use of SIRES-containing bicistronic vectors as a means to counter the downstream attenuation problem. It is still possible, in some tissue types, that the SIRES will not function well or, for some choices of the promoter type, proximal and distal genes, that the kind of results observed in the current work will not hold. Future studies will be needed to evaluate the true generalizability of the current strategy.

The incorporation of SIRES into vectors for gene therapy will allow for efficient coexpression of multiple genes from the same promoter. The 2 genes can be expressed at levels that should be able to be readily imaged in vivo. There are several approaches to link 2 genes in a single vector construct (*23*). However, there is no single approach that meets all of the criteria for a tightly correlated expression of the 2 genes. Among the different approaches, we recently used the 2-promoter approach to image the kinetics of vascular endothelial growth factor (VEGF) gene expression in ischemic myocardium (*24*). Although this approach can be used to overcome the downstream gene attenuation problems that limit the IRES approach, it also has certain limitations. The expression of the 2 genes can be uncoupled if the transcriptional activity of the 2 promoters is altered due to the inherent nature of the region where the vector integrates into the host genome. Moreover, a mutation in one or both promoters will alter their transcriptional activity. Using the SIRES vectors, we found that the expression of the downstream gene is quite robust and does not suffer from the attenuation problems commonly encountered with EMCV IRES-based vectors. The results from this study support the use of SIRES vectors for imaging gene expression in vivo. Repetitive, quantitative imaging of therapeutic gene expres-

sion based on the levels of reporter gene expression in small animal models will enable direct translation to clinical monitoring of target gene expression in patients.

CONCLUSION

We have demonstrated that SIRES-based bicistronic vectors significantly augment the levels of expression of the downstream gene using bioluminescence and microPET modalities. The development of such vectors will allow them to be used in gene therapy protocols to monitor the levels of therapeutic gene expression using imaging reporter genes.

ACKNOWLEDGMENTS

This work is supported by National Institute of Health grants P50 CA86306, SAIRP R24, and CA92865 and Department of Energy Contract DE-FC03-87ER60615.

REFERENCES

1. Tjuvajev JG, Avril N, Oku T, et al. Imaging herpes virus thymidine kinase gene transfer and expression by positron emission tomography. *Cancer Res.* 1998;58:4333–4341.
2. Gambhir SS, Barrio JR, Phelps ME, et al. Imaging adenoviral-directed reporter gene expression in living animals with positron emission tomography. *Proc Natl Acad Sci USA.* 1999;96:2333–2338.
3. Tjuvajev JG, Finn R, Watanabe K, et al. Noninvasive imaging of herpes virus thymidine kinase gene transfer and expression: a potential method for monitoring clinical gene therapy. *Cancer Res.* 1996;56:4087–4095.
4. Contag PR, Olomu IN, Stevenson DK, et al. Bioluminescent indicators in living mammals. *Nat Med.* 1998;4:245–247.
5. Contag CH, Bachmann MH. Advances in in vivo bioluminescence imaging of gene expression. *Annu Rev Biomed Eng.* 2002;4:235–260.
6. MacLaren DC, Gambhir SS, Satyamurthy N, et al. Repetitive, non-invasive imaging of the dopamine D2 receptor as a reporter gene in living animals. *Gene Ther.* 1999;6:785–791.
7. Cherry SR, Shao Y, Silverman RW, et al. MicroPET: a high resolution PET scanner for imaging small animals. *IEEE Trans Nucl Sci.* 1997;44:1161–1166.
8. Tjuvajev JG, Stockhammer G, Desai R, et al. Imaging the expression of transfected genes *in vivo. Cancer Res.* 1995;55:6126–6132.
9. Tjuvajev JG, Joshi A, Callegari J, et al. A general approach to the non-invasive imaging of transgenes using cis-linked herpes simplex virus thymidine kinase. *Neoplasia.* 1999;1:315–320.
10. Gambhir SS, Bauer E, Black ME, et al. A mutant herpes simplex virus type 1 thymidine kinase reporter gene shows improved sensitivity for imaging reporter gene expression with positron emission tomography. *Proc Natl Acad Sci USA.* 2000;97:2785–2790.
11. Iyer M, Barrio JR, Namavari M, et al. 8-[^{18}F]Fluoropenciclovir: an improved reporter probe for imaging HSV1-tk reporter gene expression in vivo using PET. *J Nucl Med.* 2001;42:96–105.
12. Ray P, Bauer E, Iyer M, et al. Monitoring gene therapy with reporter gene imaging. *Semin Nucl Med.* 2001;31:312–320.
13. Owens GC, Chappell SA, Mauro VP, et al. Identification of two short internal ribosomal entry sites selected from libraries of random oligonucleotides. *Proc Natl Acad Sci USA.* 2001;98:1471–1476.
14. Vagner S, Galy B, Pyronnet S. Irresistible IRES: attracting the translation machinery to internal ribosome entry sites. *EMBO Rep.* 2001;2:893–898.
15. Yu Y, Annala AJ, Barrio JR, et al. Quantification of target gene expression by imaging reporter gene expression in living animals. *Nat Med.* 2000;6:933–937.
16. Chappell S, Edelman G, Mauro V. A 9-nt segment of a cellular mRNA can function as an internal ribosome entry site (IRES) and when present in linked multiple copies greatly enhances IRES activity. *Proc Natl Acad Sci USA.* 2000;97:1536–1541.
17. Alauddin MM, Conti PS. Synthesis and preliminary evaluation of 9-(4-[F-18]-fluoro-3-hydroxymethylbutyl)guanine ([F-18]FHBG): a new potential imaging agent for viral infection and gene therapy using PET. *Nucl Med Biol.* 1998;25:175–180.
18. Liang Q, Satyamurthy N, Barrio JR, et al. Noninvasive, quantitative imaging in living animals of a mutant dopamine D2 receptor reporter gene in which ligand binding is uncoupled from signal transduction. *Gene Ther.* 2001;8:1490–1498.
19. Bhaumik S, Gambhir SS. Optical imaging of renilla luciferase reporter gene expression in living mice. *Proc Natl Acad Sci USA.* 2002;99:377–382.
20. Qi J, Leahy RM, Cherry SR, et al. High-resolution 3D Bayesian image reconstruction using the microPET small-animal scanner. *Phys Med Biol.* 1998;43:1001–1013.
21. Contag CH, Jenkins D, Contag PR, et al. Use of reporter genes for optical measurements of neoplastic disease in vivo. *Neoplasia.* 2000;2:41–52.
22. Wu JC, Sundaresan G, Iyer M, et al. Noninvasive optical imaging of firefly luciferase reporter gene expression in skeletal muscles of living mice. *Mol Ther.* 2001;4:297–306.
23. Sundaresan G, Gambhir SS. Radionuclide imaging of reporter gene expression. In: Toga AW, Mazziotta JC, eds. *Brain Mapping: The Methods.* San Diego, CA: Academic Press; 2002:799–818.
24. Wu JC, Chen IY, Wang Y, et al. Molecular imaging of the kinetics of vascular endothelial growth factor gene expression in ischemic myocardium. *Circulation.* 2004;110:685–691.